

Two-dimensional versus three-dimensional motion of inversion electrons in a magnetic field

J. H. Crasemann, U. Merkt, and J. P. Kotthaus

Institut für Angewandte Physik, Universität Hamburg, Jungiusstrasse 11, D-2000 Hamburg 36, West Germany

(Received 25 February 1983)

The infrared absorption of inversion electrons on InSb is measured in a magnetic field parallel to the inversion layer. The experimental results are explained by a simple model of surface electrons in crossed electric and magnetic fields. The dependence on resonance magnetic field and electron density shows a transition from two-dimensional- (2D) to 3D-like motion of the electrons.

In space-charge layers of metal-oxide-semiconductor (MOS) structures electrons are bound to the surface in electric subbands by the Coulomb force eF , perpendicular to the surface. The electrons are free to move parallel to the surface and thus form a quasi-two-dimensional (2D) electron gas.¹ In a magnetic field B parallel to the surface the electrons are also subjected to the Lorentz force that, in the limit of a 2D electron gas, acts perpendicular to the surface. In contrast to the Coulomb force, its direction depends on the direction of the electron momentum $\hbar k_y$ ($\vec{F}_s \parallel z$ and $\vec{B} \parallel x$). Accordingly, the Lorentz force will either pull the electrons into the bulk of the semiconductor, or it will bind them to the surface. The former case is energetically more favorable, and in sufficiently strong magnetic fields all electrons will eventually complete Landau circles as 3D electrons do. In the latter case, the classical trajectories are skipping orbits originating from periodic specular reflection at the surface, as is the situation in the electric limit ($B=0$).²

In the magnetic limit ($F_s=0$) the corresponding quantized surface levels have been studied at metal surfaces.³⁻⁵ On semiconductors, the combined action of the electric field and the magnetic field creates surface states that are referred to as hybrid subbands or hybrid surface levels.^{2,6} These have most extensively been studied in silicon space-charge layers^{7,8} and show an essentially 2D dispersion in a parallel magnetic field, whereas in PbTe accumulation layers 3D-like behavior has been reported.⁹

Here we demonstrate the transition from 2D- to 3D-like motion of surface electrons. As a system of investigation we have chosen InSb where the cyclotron radius can be made comparable with the spread of the subband wave function. We study the resonant infrared absorption of inversion electrons in InSb MOS structures in a magnetic field parallel to the surface. The observed spectra and their dependence on carrier concentration are explained by a model that analytically describes the transition from 2D to 3D motion in hybrid surface levels.

In this model, the electric surface potential is approximated by a triangular well potential,^{1,7} and effects of spin and nonparabolicity are neglected. In the gauge $A = (0, -Bz, 0)$, the total surface potential only depends on the z coordinate. Therefore the ansatz $U(z) \exp(ik_x x + ik_y y)$ reduces the Schrödinger equation to an equation for $U(z)$. For this, dimensionless variables are introduced by means of the cyclotron radius $l = (\hbar/eB)^{1/2}$, the cyclotron energy $\hbar\omega_c$, and the wave vector $k_D = m^*F_s/\hbar B$ that corresponds to the classical drift velocity $v_D = F_s/B$ in crossed electric and magnetic fields. The dimensionless

space coordinate is defined by

$$\zeta = \sqrt{2}(z - z_0)/l, \tag{1}$$

where $z_0 = l^2(k_y - k_D)$ turns out to be the center coordinate of the motion. A dimensionless energy parameter is defined by

$$-a = (E - E_{2D})/\hbar\omega_c + (z_0/l)^2/2, \tag{2}$$

with the 2D dispersion $E_{2D} = \hbar^2(k_x^2 + k_y^2)/2m^*$. The equation for $U(z)$ then has the standard form of the differential equation of the Weber functions.¹⁰ The motion of surface electrons thus is described by "oscillations" $U(a, \zeta)$ around z_0 . Dependent on $k_y \lesseqgtr k_D$, the center lies inside or outside the semiconductor ($z_0 \lesseqgtr 0$). The allowed energy parameters a_i ($i=0, 1, \dots$) and the hybrid subband wave functions $U(a_i, \zeta)$ follow from the boundary condition $U(a_i, z=0) = 0$. The energies in the hybrid subband i are

$$E = \frac{\hbar k_x^2}{2m^*} + \hbar\omega_c \left[-a_i + k_D l \left(\frac{k_D l}{2} + \frac{z_0}{l} \right) \right]. \tag{3}$$

The parameters a_i can be found with the aid of Fig. 1 ($k_D l = 0$) with the zeros of Weber functions taken from literature.¹⁰

Hybrid surface levels are obtained by adding $k_D l (k_D l/2 + z_0/l)$ to the $k_D l = 0$ curves (see Fig. 1). The physical meaning of the parameter $k_D l$ is illustrated by $k_D l = (l/L)^{2/3}$, $L = (\hbar^2/2m^*eF_s)^{1/3}$ being the relevant electric length of the system.¹¹ In Fig. 1, also, the corresponding abscissas $k_y l = z_0/l - k_D l$ are included. Their origin is shifted with respect to the subband minima, reflecting the diamagnetic shift.²

For center coordinates well outside the semiconductor ($z_0/l \ll -1$) the energy eigenvalues can be approximated by

$$E \approx E_{2D} + \left(\frac{9\pi^2}{8m^*} \right)^{1/3} (\hbar k_y \hbar\omega_c + \hbar eF_s)^{2/3} \left(i + \frac{3}{4} \right)^{2/3}. \tag{4}$$

Such electrons constitute a 2D electron gas. For center coordinates inside the semiconductor ($z_0/l \gg +1$) the energies

$$E \approx \frac{\hbar^2 k_x^2}{2m^*} + \hbar\omega_c \left(i + \frac{1}{2} \right) + \frac{m^* v_D^2}{2} + eF_s z_0 \tag{5}$$

of 3D electrons in crossed electric and magnetic fields are obtained.¹² At intermediate values the model describes the transition from 2D to 3D behavior. Note from Fig. 1 that at a low enough $k_D l$ value and Fermi vector k_F , taken with

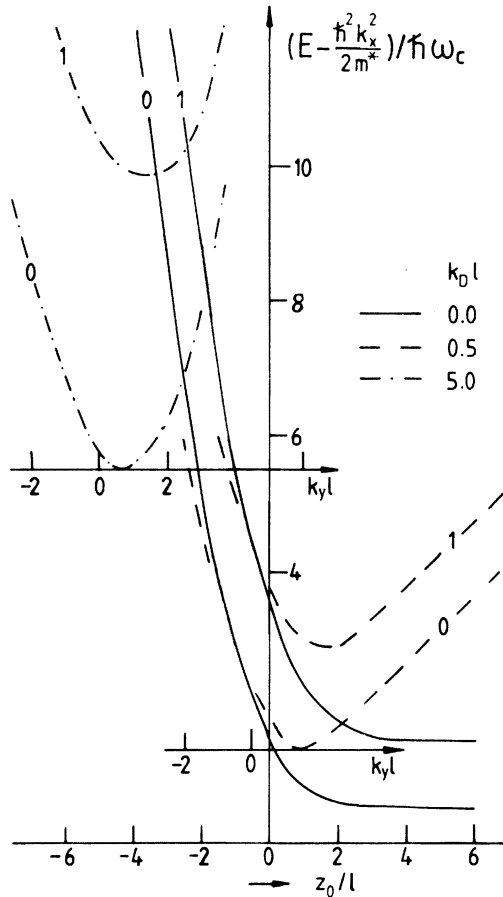


FIG. 1. Energy dispersion of hybrid subbands in parallel magnetic fields. Hybrid subbands $i=0, 1, \dots$ are obtained by adding the straight line $k_D l$ ($k_D l/2 + z_0/l$) to the purely magnetic surface levels ($k_D l=0$).

respect to the hybrid subband minimum, the center coordinates of all electrons lie inside the semiconductor and all electrons are expected to show 3D-like motion.

The experiments are performed on Ge-doped ($N_A \approx 10^{14} \text{ cm}^{-3}$) InSb(111) platelets with SiO_2 gate insulators and semitransparent NiCr gates.¹³ The absorption spectra are taken at fixed laser energies $\hbar\omega$ and inversion electron densities n_s in a sweep of the magnetic field. The far-infrared radiation is always incident perpendicular to the surface. Typical spectra taken with unpolarized light at two distinct laser energies are reproduced in Figs. 2 and 3 where the change in transmission ΔT caused by the inversion electrons is normalized to the transmission T of the sample at zero density and zero magnetic field.

Figure 2(a) for comparison presents standard surface cyclotron resonance (CR) traces, i.e., the magnetic field is perpendicular to the surface ($\theta=0$). The shift of the resonance magnetic field with density reflects the nonparabolicity of InSb subbands.¹⁴ The relatively large linewidth is mainly caused by Coulomb scattering from interface charges and surface roughness scattering.^{1,14} The small dip at $B=4.0$ T results from a bound-hole transition in the p -Insb substrate.¹⁵

The resonances observed in a parallel field are shown in Fig. 2(b) and differ drastically from the perpendicular

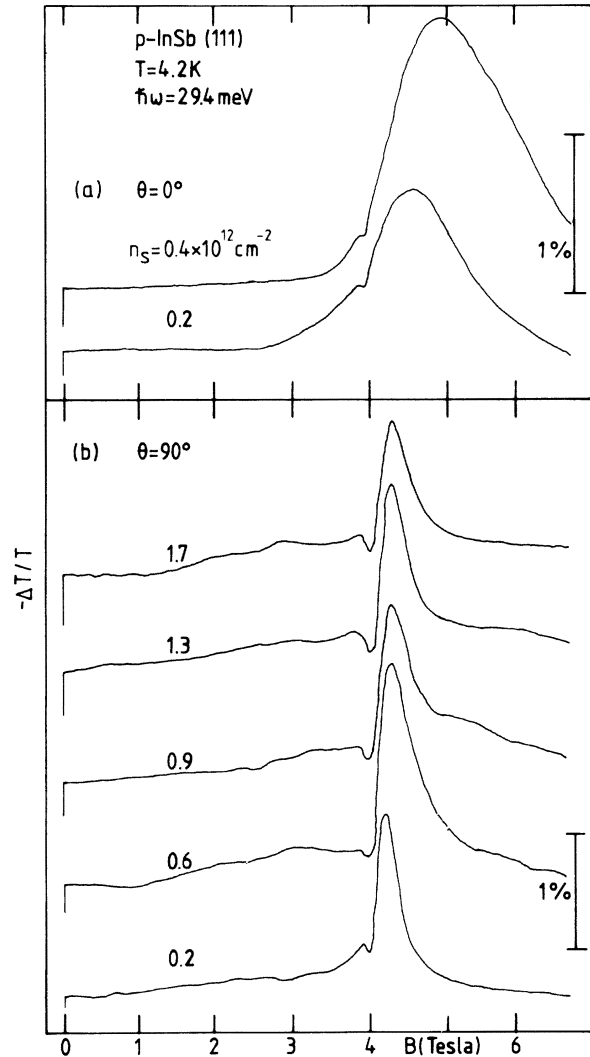


FIG. 2. Absorption spectra of inversion electrons at a laser energy $\hbar\omega=29.4$ meV. (a) Surface CR with the magnetic field perpendicular to the inversion layer ($\theta=0$). (b) Absorption in parallel magnetic fields ($\theta=90^\circ$). The traces have been successively displaced upward for clarity.

geometry [Fig. 2(a)]. The resonance position shows no noticeable shift with increasing density and agrees with the one for bulk electrons.¹⁶ The linewidth is larger than observed for bulk electrons but a factor of 5 smaller than for surface CR [$\theta=0$, Fig. 2(a)]. The broadening that is observed in Fig. 2(b) with increasing density may be caused by both increased surface scattering¹ and k_y broadening.⁵ Whereas at low density the line shape is similar to that of 3D electrons, with increasing density an essentially field-independent Drude-like contribution to the absorption occurs, which reflects additional absorption by quasi-2D electrons.

At a significantly lower excitation energy (see Fig. 3), i.e., at lower resonance magnetic fields, the spectra are qualitatively different. Two small but distinct resonance structures appear on the dominating Drude background. The resonance positions shift to higher magnetic fields with increasing density and are different from the one of bulk electrons. These characteristics are similar to those of the quasi-2D

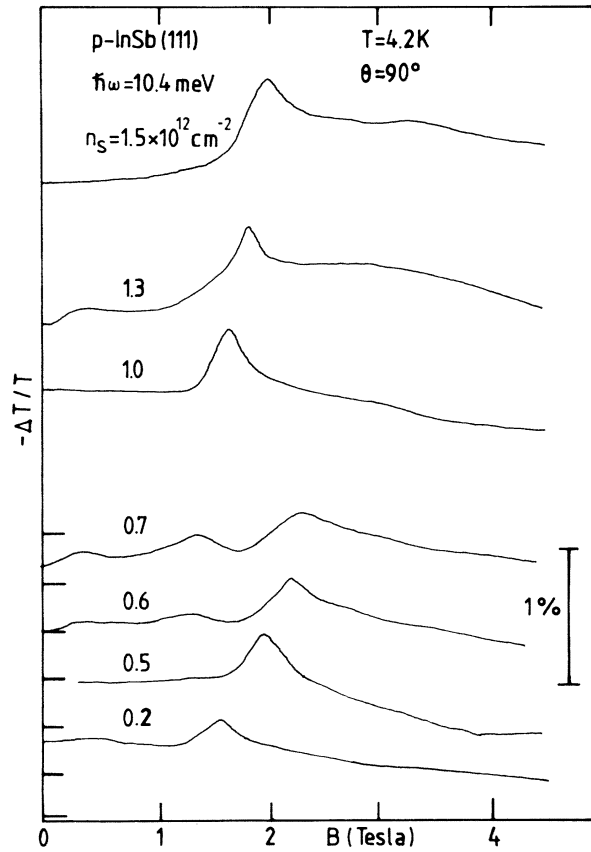


FIG. 3. Absorption spectra of inversion electrons at a laser energy $\hbar\omega = 10.4$ meV in parallel magnetic fields ($\theta = 90^\circ$). The horizontal lines at $B = 0$ mark successively the value $-\Delta T/T = 0$.

electron gas on InSb.¹⁴ We interpret the structures as caused by transitions between nonparabolic hybrid subbands. Unlike the situation in Fig. 2(b), two transitions and nonparabolicity are apparent, because the density of states decreases with decreasing magnetic field, approximately as

$$D(E) \approx m^* (1 + 0.4k_{Dl}^{-4/3})^{1/2} / \pi \hbar^2 \quad (i=0, k_{Dl} \geq 1) .$$

In experiments with linearly polarized light, the resonant structures at both laser energies are only observed in the CR active polarization. The weakly field-dependent background is not sensitive to the polarization as is, in fact, expected for Drude absorption.

Our model can semiquantitatively explain the transition from 2D to 3D behavior observed in the experimental spectra. For this, the k_{Dl} parameter is calculated with the resonant magnetic field of the corresponding conduction band CR¹⁶ and the electric field $F_s \approx en_s / \epsilon_0 \epsilon_s$.¹ The Fermi vector is approximated by $k_F \approx (2\pi n_s)^{1/2}$, provided that only one hybrid subband is occupied and $k_{Dl} \geq 1$. We expect 3D-like CR in the ground hybrid subband for inversion electrons that oscillate around positive center coordinates z_0/l . This means that the position $(z_0/l)_{\min}$ of the energy minimum in the ground hybrid subband must lie at least approximately k_{Fl} inside the semiconductor (see Fig. 1). For the lowest density studied in Figs. 2(b) and 3, one obtains $k_{Fl} = 1.3$, $(z_0/l)_{\min} = 0.8$, and $k_{Fl} = 2.5$, $(z_0/l)_{\min} = -4.0$, respectively. This explains why 3D-like CR is observed in Fig. 2(b), but not in Fig. 3.

Also by the dependence of the center coordinate $(z_0/l)_{\min}$ and Fermi vector on density, the transition to 2D behavior that is observed in Fig. 2 with increasing density can be explained. However, the observed 3D-like CR structures are astonishingly strong even at relatively high densities. To understand this feature in a quantitative way, a more realistic, screened electrostatic potential should be used and oscillator strengths must be calculated.

In conclusion, we have experimentally demonstrated the transition from 2D- to 3D-like motion of inversion electrons by their resonant infrared absorption in a parallel magnetic field. This transition is of different origin than the transition from 2D to 3D conduction by reducing the channel thickness¹⁷ and is successfully described by a simple model of hybrid surface levels that form in a magnetic field parallel to the surface.

ACKNOWLEDGMENTS

We thank F. Koch for stimulating discussions and acknowledge financial support of the Deutsche Forschungsgemeinschaft.

¹T. Ando, A. B. Fowler, and F. Stern, *Rev. Mod. Phys.* **54**, 437 (1982).

²F. Koch, in *Physics in High Magnetic Fields*, edited by S. Chikazumi and N. Miura (Springer, Berlin, 1981), pp. 262–273.

³R. E. Prange and T. W. Nee, *Phys. Rev.* **168**, 779 (1968).

⁴R. E. Doezema and J. F. Koch, *Phys. Rev. B* **5**, 3866 (1972).

⁵M. Wanner, R. E. Doezema, and U. Strom, *Phys. Rev. B* **12**, 2883 (1975).

⁶J. C. Maan, Ch. Uihlein, L. L. Chang, and L. Esaki, *Solid State Commun.* **44**, 653 (1982).

⁷W. Beinvoogl, A. Kamgar, and J. F. Koch, *Phys. Rev. B* **14**, 4274 (1976).

⁸T. Ando, *Phys. Rev. B* **19**, 2106 (1979).

⁹H. Schaber and R. E. Doezema, *Phys. Rev. B* **20**, 5257 (1979).

¹⁰J. C. P. Miller, in *Handbook of Mathematical Functions*, edited by M. Abramowitz and I. A. Stegun (Dover, New York, 1965), pp. 685–720.

¹¹S. K. Bhattacharya, *Phys. Rev. B* **25**, 3756 (1982).

¹²W. Zawadzki, in *Physics of Solids in Intense Magnetic Fields*, edited by E. D. Haidemenakis (Plenum, New York, 1969), pp. 311–328.

¹³U. Mackens and U. Merkt, *Thin Solid Films* **97**, 53 (1982).

¹⁴A. Daerr, J. P. Kotthaus, and J. F. Koch, *Solid State Commun.* **17**, 455 (1975).

¹⁵R. Kaplan, *Phys. Rev. Lett.* **20**, 329 (1968).

¹⁶J. R. Apel, T. O. Poehler, C. P. Westgate, and R. I. Joseph, *Phys. Rev. B* **4**, 436 (1971).

¹⁷D. A. Poole, M. Pepper, K. F. Berggren, G. Hill, and H. W. Myron, *J. Phys. C* **15**, 21 (1982).